JPn Neuroscience

The Journal of Physiology

J Physiol 594.10 (2016) pp 2647–2659

Zn^{2+}-induced Ca^{2+} release via ryanodine receptors triggers calcineurin-dependent redistribution of cortical neuronal Kv2.1 K^+ channels

Anthony J. Schulien[1,3], Jason A. Justice[1,3], Roberto Di Maio[2,3], Zachary P. Wills[1], Niyathi H. Shah[1] and Elias Aizenman[1,3]

[1] *Department of Neurobiology*
[2] *Department of Neurology*
[3] *Pittsburgh Institute for Neurodegenerative Diseases, University of Pittsburgh School of Medicine, PA, USA*

Key points

- Increases in intracellular Zn^{2+} concentrations are an early, necessary signal for the modulation of Kv2.1 K^+ channel localization and physiological function.
- Intracellular Zn^{2+}-mediated Kv2.1 channel modulation is dependent on calcineurin, a Ca^{2+}-activated phosphatase.
- We show that intracellular Zn^{2+} induces a significant increase in ryanodine receptor-dependent cytosolic Ca^{2+} transients, which leads to a calcineurin-dependent redistribution of Kv2.1 channels from pre-existing membrane clusters to diffuse localization. As such, the link between Zn^{2+} and Ca^{2+} signalling in this Kv2.1 modulatory pathway is established.
- We observe that a sublethal ischaemic preconditioning insult also leads to Kv2.1 redistribution in a ryanodine receptor-dependent fashion.
- We suggest that Zn^{2+} may be an early and ubiquitous signalling molecule mediating Ca^{2+} release from the cortical endoplasmic reticulum via ryanodine receptor activation.

Abstract Sublethal injurious stimuli in neurons induce transient increases in free intracellular Zn^{2+} that are associated with regulating adaptive responses to subsequent lethal injury, including alterations in the function and localization of the delayed-rectifier potassium channel, Kv2.1. However, the link between intracellular Zn^{2+} signalling and the observed changes in Kv2.1 remain undefined. In the present study, utilizing exogenous Zn^{2+} treatment, along with a selective Zn^{2+} ionophore, we show that transient elevations in intracellular Zn^{2+} concentrations are sufficient to induce calcineurin-dependent Kv2.1 channel dispersal in rat cortical neurons *in vitro*, which is accompanied by a relatively small but significant hyperpolarizing shift in the voltage-gated activation kinetics of the channel. Critically, using a molecularly encoded calcium sensor, we found that the calcineurin-dependent changes in Kv2.1 probably occur as a result of Zn^{2+}-induced cytosolic Ca^{2+} release via activation of neuronal ryanodine receptors. Finally, we couple this mechanism with an established model for *in vitro* ischaemic preconditioning and show that Kv2.1 channel modulation in this process is also ryanodine receptor-sensitive. Our results strongly suggest that intracellular Zn^{2+}-initiated signalling may represent an early and possibly widespread component of Ca^{2+}-dependent processes in neurons.

(Received 5 January 2016; accepted after revision 14 February 2016; first published online 4 March 2016)
Corresponding authors E. Aizenman or N. H. Shah: Department of Neurobiology, University of Pittsburgh School of Medicine, PA 15213, USA. Email: redox@pitt.edu; ngh7@pitt.edu

Abbreviations cER, cortical endoplasmic reticulum; Dan, dantrolene; FK520, ascomycin; GFP, green fluorescent protein; MCT, multiple comparison test; MHB, MEM-HEPES-BSA; RCaMP-h, red genetically-encoded calcium indicator protein; ROI, region of interest; RyR, ryanodine receptor; TPEN, *N,N,N',N'*-tetrakis (2-pyridylmethyl)ethane-1,2-diamine; ZnPyr, zinc-pyrithione.

DOI: 10.1113/JP272117

Introduction

Intracellular Zn^{2+} signalling is a critical regulatory component of both neurotoxic and neuroprotective cell signalling pathways. In neurons, intracellular Zn^{2+} concentrations transiently increase following exposure to a sublethal ischaemic insult (Frederickson *et al.* 2005; Aras *et al.* 2009*b*), mediating adaptive responses to subsequent excitotoxic injury. For example, chemical ischaemic preconditioning, where a sublethal ischaemic insult renders neurons resistant to subsequent lethal insults, relies heavily on intracellular Zn^{2+}-mediated signalling. Indeed, chelation of intracellular Zn^{2+} during ischaemic preconditioning attenuates the resulting neuroprotective cascade and restores cell susceptibility to excitotoxic death (Aras *et al.* 2009*b*). Conversely, lethal excitotoxic insults in neurons elicit a delayed, sustained increase in free Zn^{2+} that promotes cell death (Aras *et al.* 2009*b*; Granzotto and Sensi, 2015). Chelation of this delayed free Zn^{2+} surge supports cell survival. Taken together, these findings implicate intracellular Zn^{2+} as a regulatory component of both neuroprotective and neurodestructive cellular responses to injury (Sensi *et al.* 2011).

Injury-induced adaptive increases in intracellular free Zn^{2+} are also associated with (and indeed required for) modulation of the neuronal delayed-rectifying voltage-gated K^+ channel, Kv2.1 (Aras *et al.* 2009*a*), which localizes to highly organized somato-dendritic cell membrane-surface clusters under normal conditions (Lim *et al.* 2000; Misonou *et al.* 2004; O'Connell *et al.* 2006; Scannevin *et al.* 1996; Tamkun *et al.* 2007). Chemical ischaemic preconditioning and other injurious stimuli have been shown to alter Kv2.1 in three key modalities: (i) they induce Ca^{2+}/calmodulin-activated calcineurin-dependent dephosphorylation of the channel at multiple intracellular residues, mostly localized to the C-terminus; (ii) they induce a hyperpolarizing shift in the channel's voltage-gated activation kinetics; and (iii) they alter the distribution of Kv2.1 channels from highly localized cell membrane clusters (Lim *et al.* 2000; Misonou *et al.* 2004; O'Connell *et al.* 2006; Scannevin *et al.* 1996; Tamkun *et al.* 2007) to a more diffuse distribution throughout the neuronal plasma membrane (Du *et al.* 2000; Misonou *et al.* 2004; Misonou *et al.* 2005*a*; Mulholland *et al.* 2008; Aras *et al.* 2009*a*; Baver and O'Connell, 2012; Shepherd *et al.* 2012; Shah and Aizenman, 2014). Zn^{2+} chelation during chemical ischaemic preconditioning blocks Kv2.1 channel declustering and changes in voltage dependency (Aras *et al.* 2009*a*), suggesting a critical role for Zn^{2+} signalling in Kv2.1 modulation within the context of ischaemic injury.

Intracellular Ca^{2+} release has also been shown to play a vital role in ischaemic preconditioning-induced Kv2.1 modulation by activation of calcineurin and subsequent Kv2.1 dephosphorylation, leading to channel declustering (Misonou *et al.* 2004; Mohapatra and Trimmer, 2006; Mulholland *et al.* 2008; Aras *et al.* 2009*a*; Baver and O'Connell, 2012; Shepherd *et al.* 2012; Shah and Aizenman, 2014). However, a mechanistic link between intracellular Zn^{2+} rises, Ca^{2+} release, calcineurin activation and Kv2.1 channel modulation has yet to be firmly established. In the present study, we uncover the probable molecular pathway linking these processes, which are intimately associated with mediating neuronal tolerance and homeostatic responses to injury. Briefly, we report that the link between intracellular Zn^{2+} surges and Ca^{2+}/calcineurin-dependent modulations of Kv2.1 localization and function comprises activation of the neuronal ryanodine receptors (RyR) by intracellular Zn^{2+}. We also confirm that this RyR-dependent mechanism of Kv2.1 channel modulation is involved in the established ischaemic preconditioning pathway, which has been shown to result in neuroprotection.

Methods

Ethical approval

To generate the primary cortical neuronal cultures utilized in our experiments, one timed-pregnant, female Sprague–Dawley rat was killed each week via CO_2 inhalation, followed by exsanguination, and neuronal tissue was harvested from embryos. This procedure was carried out in accordance with The University of Pittsburgh Institutional Animal Care and Use Committee and the policies and regulations outlined in 'Principles and standards for reporting animal experiments in *The Journal of Physiology* and *Experimental Physiology*' (Grundy, 2015). The investigators understand the ethical principles under which the journal operates and have complied with these standards.

Cell culture, transfection and drug treatments

All experiments utilized primary cortical neurons cultured from embryonic day 17 Sprague–Dawley rats of either sex (Hartnett *et al.* 1997). Transfections were performed 21–25 days *in vitro* using Lipofectamine 2000 (Invitrogen, Carlsbad, CA, USA) (Aras *et al.* 2009*b*). Briefly, neuronal cultures were treated with 1.5 μg of total DNA, 2 μl of Lipofectamine 2000 and 100 μl of Opti-MEM (Gibco, Grand Island, NY, USA) per well. Cells were utilized for experimentation ~18–24 h following transfection. Treatment solutions were prepared in modified Minimal Essential Media (Life Technologies, Carlsbad, CA, USA), which contained 25 mM Hepes and 0.01% BSA (MHB). MHB media was utilized for both treatments and imaging to avoid media change-triggered Kv2.1 declustering (Fox *et al.* 2015).

Confocal imaging

For analysis of transfected Kv2.1-GFP channel distribution, neuronal cultures were imaged on a A1+ confocal microscope (Nikon, Tokyo, Japan) at 60× magnification. Between five and 15 optical sections (0.5 μm) were obtained to generate a maximum intensity projection image for visualizing Kv2.1 surface clusters as described earlier (Shah *et al.* 2014). Utilizing Nikon Instruments Software Elements Advanced Research (NIS-Elements AR) analysis, the object count feature was customized to analyse metrics on Kv2.1 clusters. Object count parameters defined a Kv2.1 cluster as an area of high intensity green fluorescent protein (GFP) signal (compared to background) measuring 0.05 μm^2 or larger (Shah *et al.* 2014). NIS-Elements AR was also utilized to measure the somatic area of each neuron to calculate a normalized value of Kv2.1 clusters/μm^2 of neuronal soma.

Calcium imaging

To test the capability of intracellular Zn^{2+} to induce cytosolic Ca^{2+} release, neuronal cultures were transfected with a GFP-n1 construct (85% of total DNA) to visualize neurons in their entirety, as well as a genetically-encoded Ca^{2+} sensor, red genetically-encoded calcium indicator protein (RCaMP-h) (15% of total DNA) to measure intracellular Ca^{2+} release signals. Upon translation, RCaMP-h binds intracellular Ca^{2+} ions with high affinity and emits red fluorescence when excited by 561 nm light (Akerboom *et al.* 2013). Thus, RCaMP-h fluorescence measurements provided visual confirmation of intracellular Ca^{2+} events. Eighteen to 24 h post-transfection, neuronal cultures on glass coverslips were loaded into an imaging chamber with 0.5 ml of MHB. Neurons were imaged on a A1+ confocal microscope at 60× magnification. Cells were imaged continuously over a total period of ∼20 min, and drug solutions were directly infused into the imaging chamber following baseline fluorescence measurements for ∼10 min. During experiments, both RCaMP-h and GFP fluorescence measurements from the neuronal soma were recorded with respect to time. Increases in red light emission, relative to GFP fluorescence emission, correlated with RCaMP-h-Ca^{2+} binding, indicating that cytosolic Ca^{2+} had been liberated near the transfected protein. Traces (e.g. Fig. 4) are shown as the ratio of background-corrected RCaMP-h/GFP fluorescence *vs.* time. To analyse Ca^{2+} event frequency, the first derivative plot of each RCaMP-h/GFP trace was obtained using MatLab (MathWorks Inc., Natick, MA, USA), eliminating major background fluctuations in RCaMP-h fluorescence. A period of baseline quiescence (15–20 s) was defined for the 10 min segments prior to and following drug infusion. A Ca^{2+} transient was considered as an area on the first derivative plot that spanned 3 SDs above and below the established baseline level, indicating a rise and fall of the RCaMP-h emission signal slope.

Zinc imaging

To confirm that Zn^{2+} permeated the neuronal membrane during zinc-pyrithione (ZnPyr) treatment (30 μM $ZnCl_2$, 300 nM pyrithione), a highly selective, cell-permeant, Zn^{2+}-sensitive molecular probe, FluoZin3-AM (Life Technologies, Carlsbad, CA, USA) was utilized. Neurons were first loaded with FluoZin3-AM (10 μM for 30 min) prepared in a Hepes buffered salt solution (144 mM NaCl, 3 nM KCl, 10 mM Hepes, 5.5 mM glucose, pH 7.3). Following incubation at 37°C and 5% CO_2 with the probe, neuronal cultures were washed with MHB, and immediately transferred to an imaging chamber containing 2.5 ml MHB. Neurons were imaged on a DMIRB microscope (Leica Microsystems, Wetzlar, Germany) at 20× magnification. Neurons within an imaging field (n = 10–20) were excited with 490 nm light every 10 s until baseline fluorescence levels stabilized. ZnPyr treatments were directly infused into the imaging chamber during continuous imaging. Following free Zn^{2+} increases, a cell-permeant Zn^{2+} chelator, *N*,*N*,*N*',*N*'-tetrakis(2-pyridylmethyl)ethane-1,2-diamine (TPEN; 20 μM), was utilized to decrease Zn^{2+} fluorescence signal and confirm its Zn^{2+}-dependency.

Electrophysiology

Whole-cell voltage clamp currents were obtained with an Axopatch 200B amplifier and pClamp software (Molecular Devices, LLC., Silicon Valley, CA, USA) using 3–5 MΩ electrodes. Whole-cell K^+ currents were measured immediately before and after application of either ZnPyr (30 μM $ZnCl_2$, 300 nM pyrithione) or ZnPyr + dantrolene (Dan) (30 μM $ZnCl_2$, 300 nM pyrithione, 10 μM Dan) in an extracellular recording solution (115 mM NaCl, 2.5 mM KCl, 2.0 mM $MgCl_2$, 1.0 mM $CaCl_2$, 10 mM Hepes, 10 mM D-glucose and 0.25 μm tetrodotoxin, pH 7.2). The electrode solution contained 100 mM K-gluconate, 10 mM KCl, 1 mM $MgCl_2$, 1 mM $CaCl_2$, 2.2 mM Mg_2·ATP, 0.33 mM GTP, 11 mM EGTA and 10 mM Hepes (pH 7.2). Series resistance was partially compensated (80%) in all cases. Currents were filtered at 2 kHz and digitized at 10 kHz. K^+ currents were evoked with a series of 200 ms voltage steps from a holding potential of −80 to +80 mV in 10 mV increments. Before depolarization, a single 30 ms pre-pulse to +10 mV was used to inactivate A-type K^+ currents. Conductance (G) was calculated from peak steady-state current amplitudes (I) using the equation $G = I/(V - E_K)$. G/G_{max} was plotted against the membrane potential and fit to a Boltzmann function, $G = G_{max}/(1 + \exp[-(V - V_{1/2})/k])$, where $V_{1/2}$

is the voltage of half-maximal activation and k is the slope factor of activation.

Chemical ischaemic preconditioning

Following transfection with a GFP-tagged Kv2.1 construct (to enable visualization of Kv2.1 localization during microscopy), cortical neurons *in vitro* were pre-treated for 20 min with either vehicle (DMSO) or ryanodine [15 μM ryanodol 3-(^{1}H-pyrrole-2-carboxylate)] solutions, made up in a glucose-free balanced salt solution (150 mM NaCl, 2.8 mM KCl, 1 mM $CaCl_2$, 10 mM Hepes, pH 7.2). Following pre-treatment, cells were preconditioned for 90 min with 3 mM KCN (or ddH_2O) accompanied by either vehicle (DMSO) or ryanodine co-treatment, following a protocol similar to that described in Aras *et al.* (2009*b*). After ischaemic preconditioning, coverslips were washed with solutions identical to pre-treatments. Kv2.1 localization was analysed via confocal microscopy immediately following preconditioning or vehicle-treatment. Confocal image acquisition followed a protocol similar to that described above.

Statistical analysis

All data are presented as the mean ± SEM. All statistical analyses were performed in PRISM (GraphPad Software Inc., San Diego, CA, USA). When more than two means were compared, a one-way ANOVA was utilized with Dunnett's multiple comparison test (MCT) *vs.* vehicle or control-treated group. Sets of paired observations or experiments only involving two groups were analysed via two-tailed t tests. α was set at 0.05 for experiments (95% confidence). $P < 0.05$ was considered statistically significant.

Results

Intracellular Zn^{2+} increases are sufficient to induce transient Kv2.1 channel declustering

Preconditioning-induced, sublethal increases in intracellular Zn^{2+} concentrations are sufficient to induce neuronal tolerance and associated Kv2.1 modulations in neurons (Aras *et al.* 2009*b*; Aras *et al.* 2009*a*). Furthermore, we have previously shown that preconditioning-induced Kv2.1 channel cluster dispersal is inhibited by chelation of intracellular Zn^{2+} surges produced by the injurious treatment (Aras *et al.* 2009*a*). Thus, we first examined whether rises in intracellular Zn^{2+} alone were sufficient to induce Kv2.1 channel declustering, aiming to more closely associate intracellular Zn^{2+} signalling with induction of the Kv2.1 modulation process. To accomplish this, neurons were transfected with a GFP-tagged Kv2.1 construct, which produces somatodendritic Kv2.1 channel clusters similar to endogenous channels (Misonou *et al.* 2004; O'Connell *et al.* 2006; Shah *et al.* 2014), to visualize channel distribution. Treatment with exogenous Zn^{2+} in combination with the selective Zn^{2+} ionophore, pyrithione (ZnPyr; 30 μM $ZnCl_2$, 300 nM pyrithione), for 2 h facilitated a surge in intracellular Zn^{2+} (Aras *et al.* 2009*b*). This concentration of Zn^{2+} has been shown to provide neuroprotection in previous studies and thus serves as an appropriate model for preconditioning-induced intracellular Zn^{2+} increases (Aras *et al.* 2009*b*). We found that the ZnPyr treatment yielded significant reduction of Kv2.1 clustering compared to vehicle (300 nM pyrithione)-treated cells (Vehicle, 0.155 ± 0.011 Kv2.1 clusters/μm^2 of neuronal soma, $n = 25$; ZnPyr 2 h, 0.093 ± 0.015 Kv2.1 clusters/μm^2, $n = 14$) (Fig. 1*A* and *B*).

In previous studies, Kv2.1 channel clusters returned to their clustered state 24 h following withdrawal of the preconditioning stimulus (Aras *et al.* 2009*a*; Shah *et al.* 2014). To investigate whether Zn^{2+}-induced channel declustering was also transient, we imaged neuronal cultures 24 h following the 2 h ZnPyr treatment (Fig. 1*A*) and found that Kv2.1 clusters were predominantly restored compared to vehicle-treated neurons (ZnPyr 26 h, 0.116 ± 0.014 Kv2.1 clusters/μm^2, $n = 15$) (Fig. 1*A* and *B*).

Next, we confirmed that Zn^{2+} mediated its effect primarily by an intracellular mechanism, and not by binding to the extracellular, ligand-binding domain of the metabotropic Zn^{2+} receptor mZnR/GPR39 (Besser *et al.* 2009), or by mediating some other extracellular signalling-dependent process. We removed pyrithione from the treatment solution, thereby preventing Zn^{2+} entry into the neuronal cytosol, and proceeded with Kv2.1 cluster imaging following Zn^{2+} exposure for 2 h (Zn; 30 μM $ZnCl_2$). No significant level of declustering was displayed in this case (Fig. 1*A*), confirming that Zn^{2+}-dependent Kv2.1 channel declustering effect is indeed mediated by an intracellular, Zn^{2+}-activated signalling pathway (Zn 2 h, 0.162 ± 0.011 Kv2.1 clusters/μm^2, $n = 16$) (Fig. 1*B*).

To confirm the efficacy of pyrithione in facilitating Zn^{2+} influx during the ZnPyr treatments, especially because our incubating solution contained phosphate, a possible Zn^{2+}-binding media component, Zn^{2+} imaging was carried out using the Zn^{2+}-sensitive cell-permeant probe, FluoZin3-AM. ZnPyr treatment during live imaging of neuronal somas (region of interest; ROI) yielded significant increases in FluoZin3-AM fluorescence ($n = 15$ cells), which were attenuated by addition of the selective Zn^{2+} chelator TPEN (20 μM) (Fig. 1*C*). Although we had not expected any precipitation of free Zn^{2+} in our media based on the published solubility product of $Zn_3(PO_4)_2$ (Yamasaki *et al.* 2012), this experiment confirms that our experimental conditions are adequate for inducing intracellular increases in free Zn^{2+}.

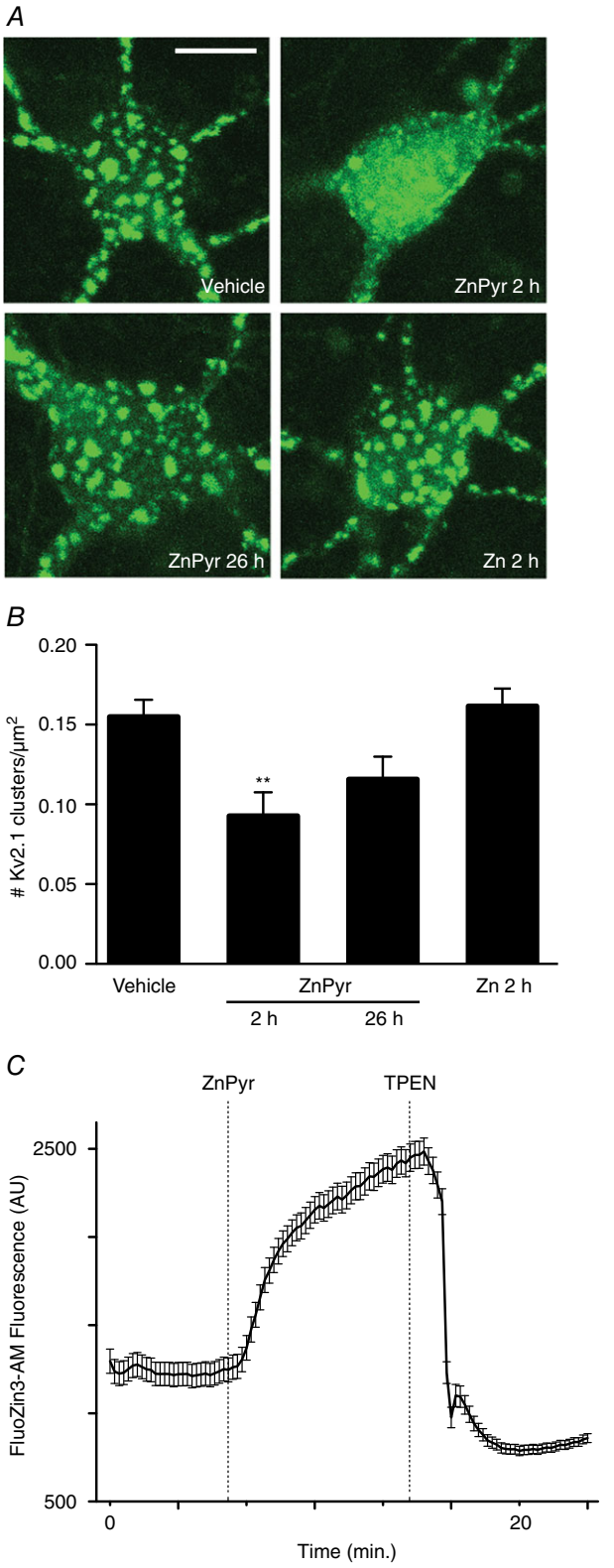

Figure 1. Sublethal elevation of intracellular Zn^{2+} concentration induces transient Kv2.1 channel cluster dispersal in neurons
A, confocal images of cortical neurons transfected with a GFP-tagged Kv2.1 construct, representative of Kv2.1 localization following treatment with either vehicle (ddH_2O, 300 nM pyrithione), ZnPyr (30 μM $ZnCl_2$, 300 nM pyrithione) or Zn (30 μM $ZnCl_2$) conditions. ZnPyr-treated neurons are shown both immediately and 24 h following 2 h treatment. Scale bar = 10 μm. *B*, showing the mean number of Kv2.1 clusters found in each condition, normalized to neuronal somatic area (number of Kv2.1 clusters μm^{-2} of neuronal soma). Data are are shown for each condition as the mean ± SEM (Vehicle, 0.155 ± 0.011, $n = 25$; ZnPyr 2 h, 0.093 ± 0.015, $n = 14$; ZnPyr 26 h, 0.116 ± 0.014, $n = 15$; Zn 2 h, 0.162 ± 0.011, $n = 16$). Analysed via one-way ANOVA with Dunnett's MCT *vs.* vehicle-treated neurons (**$P < 0.01$). *C*, trace represents Zn^{2+} entry into neurons as a function of FluoZin3-AM (a cell-permeant, Zn^{2+}-sensitive probe) fluorescence (AU) *vs.* time (min). ZnPyr was infused ~7 min following baseline measurement, whereas TPEN, a cell-permeant Zn^{2+} chelator was infused at ~14 min, to confirm the Zn^{2+}-dependency of FluoZin3-AM fluorescence. Data points are shown as the mean ± SEM of fluorescence measurements (AU) for $n = 15$ cell ROIs measured in the experiment.

Zn^{2+}-induced Kv2.1 channel declustering is critically dependent on calcineurin activation

Similar to increases in intracellular Zn^{2+}, calcineurin-mediated Kv2.1 channel dephosphorylation is also required for ischaemic preconditioning-induced channel declustering (Misonou *et al.* 2005*b*; Mohapatra and Trimmer, 2006; Aras *et al.* 2009*b*; Aras *et al.* 2009*a*; Shah *et al.* 2014). Thus, we hypothesized that calcineurin activation may be critically linked to Zn^{2+}-induced Kv2.1 channel declustering as well. To test this hypothesis, we co-treated neurons with ZnPyr in the presence of ascomycin (FK520) (5 μM), a potent inhibitor of calcineurin activity (Lotem *et al.* 1999; Shah *et al.* 2014) for 2 h. Indeed, calcineurin antagonism during ZnPyr treatment completely prevented Zn^{2+}-induced Kv2.1 declustering because neurons presented prominent clusters similar to vehicle-treated neurons (Fig. 2*A*). FK520 alone had no effect on basal Kv2.1 clustering levels (Vehicle, 0.141 ± 0.014 Kv2.1 clusters/μm^2, $n = 20$; ZnPyr 2 h, 0.072 ± 0.008 Kv2.1 clusters/μm^2, $n = 41$; ZnPyr + FK520 2 h, 0.168 ± 0.014 Kv2.1 clusters/μm^2, $n = 24$; FK520 2 h, 0.147 ± 0.020 Kv2.1 clusters/μm^2, $n = 9$) (Fig. 2*B*).

RyR activity is vital to Zn^{2+}-induced Kv2.1 channel declustering and functional modulations

In the previous experiments, we confirmed an association between surges in intracellular Zn^{2+} concentrations and calcineurin activation. Next, we aimed to characterize a possible mechanistic link between free Zn^{2+} elevations and subsequent cytosolic Ca^{2+} liberation required for calcineurin activation. We hypothesized that this mechanism may rely on RyRs, large intracellular receptors situated on subsurface cisternae of the cortical endoplasmic reticulum (cER), which allow Ca^{2+} ion liberation

from cER stores when open. Recent studies have noted close apposition between Kv2.1 channel clusters and neuronal RyR clusters of similar morphology, situated on the cER (Mandikian *et al.* 2014). Furthermore, functional junctions appear to exist between Kv2.1 clusters and the cER, with changes in cER association with the plasma membrane correlating closely with changes in Kv2.1 localization (Fox *et al.* 2015). Importantly, intracellular Zn^{2+} has also been noted to directly modulate RyR2 in cardiac myocytes, acting as a primary agonist stimulating Ca^{2+} release at low micromolar concentrations (Woodier *et al.* 2015). Moreover, Zn^{2+} action via RyR or IP3-mediated pathways may modulate intracellular neuronal Ca^{2+} levels (Johanssen *et al.* 2015), although the mechanistic details behind this process have not been directly demonstrated. Given this evidence and our present findings, we hypothesized that intracellular Zn^{2+}-dependent calcineurin activation and consequent Kv2.1 modulations probably rely on RyR activation-dependent liberation of cytosolic Ca^{2+}.

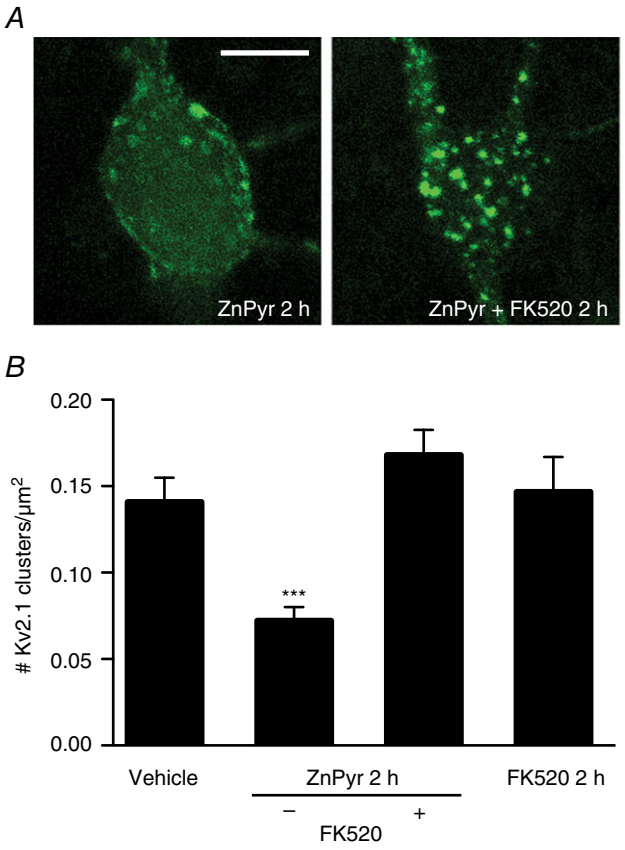

Figure 2. Intracellular Zn^{2+}-induced Kv2.1 channel dispersal is calcineurin-dependent
A, confocal images of cortical neurons transfected with a GFP-tagged Kv2.1 construct, representative of Kv2.1 localization following treatment with either ZnPyr (30 μM $ZnCl_2$, 300 nM pyrithione) or ZnPyr + FK520 (30 μM $ZnCl_2$, 300 nM pyrithione, 5 μM FK520) conditions for 2 h. Control images not relevant to this finding were omitted; both vehicle-treated and FK520-treated neurons showed significant Kv2.1 channel clustering. Scale bar = 10 μm. *B*, showing the mean number of Kv2.1 clusters found in each condition, normalized to neuronal somatic area (number Kv2.1 clusters μm^{-2} of neuronal soma). Data are shown for each condition as the mean ± SEM (Vehicle, 0.141 ± 0.014, $n = 20$; ZnPyr 2 h, 0.072 ± 0.008, $n = 41$; ZnPyr + FK520 2 h, 0.168 ± 0.014, $n = 24$; FK520 2 h, 0.147 ± 0.020 Kv2.1, $n = 9$). Analysed via one-way ANOVA with Dunnett's MCT *vs.* vehicle-treated neurons (***$P < 0.001$).

To investigate this potentially novel mechanism of intracellular Ca^{2+} release in neurons, we first examined the effects of RyR inhibition on Zn^{2+}-induced Kv2.1 channel cluster dispersal. We co-treated neurons during ZnPyr treatment with the RyR antagonist dantrolene (Dan; 10 μM). In our first set of studies, we found that this concentration of Dan was somewhat toxic to neurons over a 2 h treatment, and thus decreased our exposure to 1 h. We thus needed to confirm that the ZnPyr-induced Kv2.1 channel declustering still occurred at this time-point, which was indeed the case (Vehicle, 0.201 ± 0.034 Kv2.1 clusters/μm^2, $n = 8$; ZnPyr 1 h, 0.067 ± 0.011 Kv2.1 clusters/μm^2, $n = 20$) (Fig. 3*A* and *B*). Importantly, the addition of Dan to the ZnPyr treatment significantly attenuated Zn^{2+}-induced declustering (ZnPyr + Dan 1 h, 0.156 ± 0.026 Kv2.1 clusters/μm^2, $n = 10$) (Fig. 3*A* and *B*), supporting a role for RyR activation in Zn^{2+}-mediated Kv2.1 channel modulation. Additionally, we performed a similar experiment using ryanodine [15 μM ryanodol 3-(1H-pyrrole-2-carboxylate)], which inhibits RyR activity at micromolar concentrations (Sutko *et al.* 1997). Similar to Dan treatment, ryanodine-mediated inhibition of RyR activity also significantly attenuated Zn^{2+}-induced Kv2.1 declustering (ZnPyr + ryanodine 1 h, 0.195 ± 0.044 Kv2.1 clusters/μm^2, $n = 8$) (Fig. 3*A* and *B*). Neither ryanodine, nor Dan (with pyrithione vehicle) alone affected basal Kv2.1 channel clustering status (Vehicle + Dan/pyrithione 1 h, 0.173 ± 0.018 Kv2.1 clusters/μm^2, $n = 9$; Vehicle + ryanodine 1 h, 0.161 ± 0.019 Kv2.1 clusters/μm^2, $n = 6$) (Fig. 3*B*). These results strongly suggest that the missing link between surges in intracellular Zn^{2+} and calcineurin activation, resulting in Kv2.1 modulation and changes in localization, may lie within the activation of neuronal RyR to cause Ca^{2+} release.

Activation of calcineurin by intracellular Ca^{2+} and subsequent dephosphorylation of Kv2.1 are also known to shift the activation voltage of the channel in a hyperpolarizing direction (Park *et al.* 2006). Although a previous, non-paired design study conducted in our laboratory failed to observe a measurable shift in the activation voltage of Kv2.1 in ZnPyr-treated neurons compared to vehicle-treated cells (Aras *et al.* 2009*a*), we revisited this issue and measured K^+ currents in the same neurons before and after the addition of

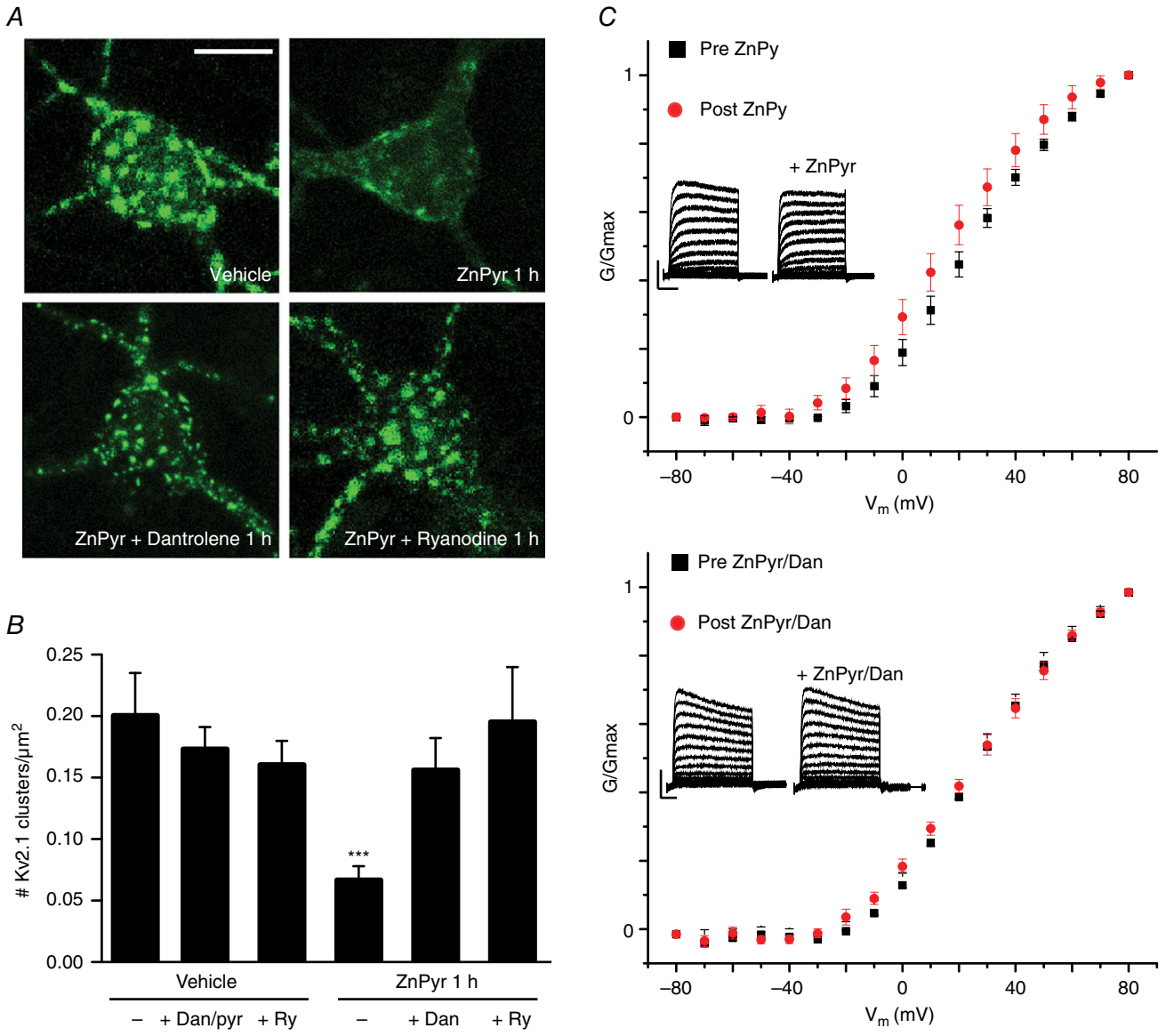

Figure 3. Intracellular Zn^{2+}-induced Kv2.1 channel dispersal is critically reliant on intermediate neuronal RyR activity

A, confocal images of cortical neurons transfected with a GFP-tagged Kv2.1 construct, representative of Kv2.1 localization following treatment with either vehicle (ddH_2O/DMSO), ZnPyr (30 μM $ZnCl_2$, 300 nM pyrithione), ZnPyr + Dan (30 μM $ZnCl_2$, 300 nM pyrithione, 10 μM Dan) or ZnPyr + ryanodine (30 μM $ZnCl_2$, 300 nM pyrithione, 15 μM ryanodine) conditions for 1 h. Control images not relevant to this finding are not shown; Dan and ryanodine only-treated neurons showed significant Kv2.1 channel clustering. Scale bar = 10 μm. *B*, showing the mean number of Kv2.1 clusters found in each condition, normalized to neuronal somatic area (number of Kv2.1 clusters μm^{-2} of neuronal soma). Data are shown for each condition as the mean ± SEM (Vehicle, 0.201 ± 0.034, $n = 8$; Vehicle + Dan/pyrithione 1 h, 0.173 ± 0.018, $n = 9$; Vehicle + ryanodine 1 h, 0.161 ± 0.019, $n = 6$; ZnPyr + vehicle 1 h, 0.067 ± 0.011 Kv2.1, $n = 20$; ZnPyr + Dan 1 h, 0.156 ± 0.026, $n = 10$; ZnPyr + ryanodine 1 h, 0.195 ± 0.044, $n = 8$). Analysed via one-way ANOVA with Dunnett's MCT *vs.* vehicle-treated neurons (***$P < 0.001$). *C*, top: average normalized *G–V* relationship of peak K^+ currents is shown as the mean ± SEM, for all neurons before (black) and after (red) ZnPyr addition. Average half-maximal activation voltage values (mV) were calculated for statistical analysis (pre-ZnPyr, 24.15 ± 2.72 mV; post-ZnPyr, 18.06 ± 3.29 mV; $n = 9$; $P < 0.01$); bottom: the same trend before and after ZnPyr + Dan treatment (pre-ZnPyr + Dan, 19.92 ± 4.21 mV; post-ZnPyr + Dan, 16.81 ± 5.39 mV; $n = 7$; (n.s.). Both paired data sets analysed via paired *t* test (two-tailed). Below: Inlays representative whole-cell current traces before and after each treatment condition. Scale bar: vertical = 2000 pA; horizontal = 60 ms.

ZnPyr to the culture bath. Under these conditions, we were able to observe a small but statistically significant, hyperpolarizing shift in the half-maximal activation voltage (pre-ZnPyr, 24.15 ± 2.72 mV; post-ZnPyr, 18.06 ± 3.29 mV, $n = 9$) (Fig. 3*C*) during these paired studies. Importantly, Dan inhibition of RyR during ZnPyr treatment was sufficient to abolish the magnitude and significance of the voltage activation shift (pre-ZnPyr + Dan, 19.92 ± 4.21 mV; post-ZnPyr + Dan, 16.81 ± 5.39 mV, $n = 7$) (Fig. 3*C*), indicating that the small level of hyperpolarizing shift in Kv2.1 activation kinetics induced by intracellular Zn^{2+} relies on RyR activation as well.

Intracellular Zn^{2+} induces a RyR-dependent increase in cytosolic Ca^{2+} release event frequency

Because our results suggest Zn^{2+}-induced Kv2.1 channel modulation to be critically dependent on the neuronal RyR, we investigated the possibility that Zn^{2+} may be directly modulating these receptors to increase intracellular Ca^{2+} liberation. Evidence of this phenomenon has been demonstrated in cardiac cells (Woodier *et al.* 2015) but has not yet been explored as a physiological process in neurons. A demonstration of this process would provide the critical link between Zn^{2+} and Ca^{2+}/calcineurin dependency of Kv2.1 modulation.

To test this hypothesis, we co-transfected cortical neurons *in vitro* with a GFP-n1 plasmid to visualize neurons, along with a genetically encoded Ca^{2+}-sensitive fluorophore, RCaMP-h, aiming to visualize and measure intracellular Ca^{2+} release in real time, before and after direct ZnPyr infusion into imaging media. In control cells, many neurons displayed spontaneous Ca^{2+} release events, correlating with an increased fluorescence produced by RCaMP-h. These release events usually lasted 2–4 s and ranged in magnitude from focal fluorescence in compartmentalized areas of the cell to global release with stronger RCaMP-h signal production (Fig. 4*A*). Following ZnPyr infusion, a significant 96% increase in measurable Ca^{2+} event frequency occurred, on average (pre-ZnPyr, 0.84 ± 0.23 Ca^{2+} transients/min; post-ZnPyr, 1.65 ± 0.37 Ca^{2+} transients/min, $n = 10$) (Fig. 4*C*). These results suggest that intracellular Zn^{2+} can indeed increase intracellular Ca^{2+} levels, or at least influence the frequency of cytosolic Ca^{2+} release events.

To test whether Zn^{2+} was acting through RyR to cause intracellular Ca^{2+} liberation, we first attempted to treat the cells with Dan (10 μM) both before and during ZnPyr infusion. We found that Dan almost completely quenched the RCaMP-h signal prior to ZnPyr addition, without affecting GFP fluorescence. Although we have no explanation for this phenomenon, we did identify a study suggesting that calmodulin significantly potentiates the actions of Dan in blocking RyR isoforms (Gomez-Hurtado *et al.* 2014). Because the RCaMP-h protein comes from a family of proteins derived from calmodulin (Akerboom *et al.* 2013), Dan may have just simply interacted with the fluorescent Ca^{2+} sensor to abolish its signal. Regardless, under these circumstances, we felt that using Dan in these experiments might yield erroneous conclusions. Accordingly, we turned our attention again to ryanodine itself, which, as mentioned earlier, is known to inhibit RyR at micromolar concentrations (Sutko *et al.* 1997) and, as shown in the present study, can block ZnPyr-mediated Kv2.1 cluster dispersal in a fashion similar to Dan (Fig. 3*A*). In our experiments described below ($n = 8$), we found that baseline RCaMP-h fluorescence was not affected by ryanodine (15 μM), enabling us to use and interpret the results of this experiment (i.e. based on the data generated below, baseline fluorescence measurements appeared to be unaffected upon the addition of ryanodine to the imaging chamber). Importantly, both spontaneous and Zn^{2+}-induced Ca^{2+} release events were significantly reduced by ryanodine application (Fig. 4*B* and *C*). Neurons treated with ryanodine showed, on average, just an 8% increase in Ca^{2+} release events following ZnPyr infusion (pre-ZnPyr + ryanodine, 0.43 ± 0.15 Ca^{2+} transients/min; post-ZnPyr + ryanodine, 0.47 ± 0.20 Ca^{2+} transients/min, $n = 8$, ns) (Fig. 3*C*) compared to the 96% increase following ZnPyr infusion alone. These results strongly suggest that intracellular Zn^{2+} causes Ca^{2+} liberation from the cER and subsequent calcineurin activation via a RyR-dependent mechanism.

Neuronal RyR inhibition attenuates chemical ischaemic preconditioning-mediated Kv2.1 channel cluster dispersal

Chemical ischaemic preconditioning with KCN (3 mM) has been shown to induce a rapid, transient increase in intracellular Zn^{2+} concentration within neurons that results in Kv2.1 channel declustering and concomitant neuronal tolerance to subsequent lethal excitotoxic stimuli (Aras *et al.* 2009*a*). We thus tested whether preconditioning-induced changes in Kv2.1 were also dependent on RyR activation. Note that, in these experiments, we also utilized ryanodine (15 μM) as our primary RyR antagonist because the combination of KCN and Dan proved to be highly toxic to the cells. We found that RyR antagonism during chemical ischaemic preconditioning treatment significantly attenuated the dispersal of Kv2.1 channel clusters induced by the KCN treatment alone (Vehicle, 0.190 ± 0.014 Kv2.1 clusters/μm^2, $n = 11$; KCN, 0.081 ± 0.025 Kv2.1 clusters/μm^2, $n = 11$; KCN + ryanodine, 0.169 ± 0.032 Kv2.1 clusters/μm^2, $n = 10$) (Fig. 5).

Overall, these results suggest that chemical ischaemic preconditioning stimuli mediate changes in Kv2.1

localization and function by a Zn^{2+}/Ca^{2+} co-dependent pathway, which is critically reliant on the Ca^{2+}-releasing activity of neuronal RyRs. These results firmly establish neuronal RyR activation as the missing link between intracellular Zn^{2+} surges and Ca^{2+}-dependent processes in Kv2.1 modulation following preconditioning, and possibly by other sublethal injurious processes that result in increases in intracellular Zn^{2+}.

Discussion

Intracellular Zn^{2+} signalling is a critical step in the modulation of Kv2.1 channel function and the activation of associated neuroprotective mechanisms in neurons (Aras *et al.* 2009*b*; Aras *et al.* 2009*a*). As such, Zn^{2+} has been shown to be essential to the chemical ischaemic preconditioning process, as well as to the associated alterations in Kv2.1 channel localization and voltage-gated activation kinetics. Furthermore, Ca^{2+}/calcineurin-dependent dephosphorylation of the channel is an important step in modulating Kv2.1 in response to a wide range of injurious processes (Misonou *et al.* 2004; Surmeier and Foehring, 2004; Mulholland *et al.* 2008; Aras *et al.* 2009*b*; Mohapatra *et al.* 2009; Baver and O'Connell, 2012; Shepherd *et al.* 2012; Shah and Aizenman, 2014). However, the link between Zn^{2+} and Ca^{2+} in this important adaptive neuronal process has not been established previously.

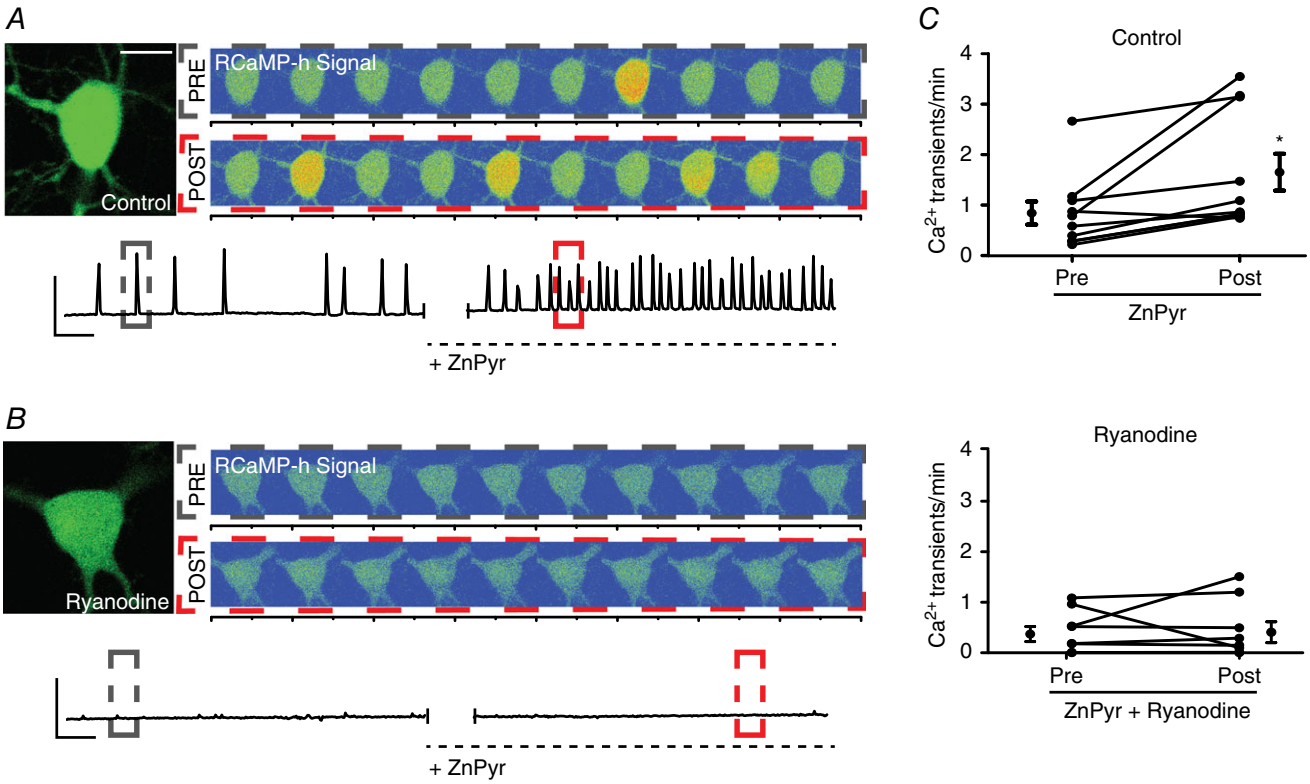

Figure 4. Sublethal surges in intracellular Zn^{2+} concentration trigger an increase in cytosolic Ca^{2+} release via neuronal RyR modulation
A, cortical neuron transfected with GFP-n1 and RCaMP-h plasmid. Left: GFP-only image; scale bar = 10 μm. Right: two sets of images are shown representative of 40 s segments of RCaMP-h fluorescence measurements in a representative neuron, correlating with cytosolic Ca^{2+} binding to expressed intracellular RCaMP-h protein. Images are shown with a rainbow-contrast filter to increase visibility of live intracellular Ca^{2+} release events (red-orange surges). The top set of images represents Ca^{2+} events pre-ZnPyr (30 μM $ZnCl_2$, 300 nM pyrithione) infusion, whereas the bottom set reflects Ca^{2+} events post-ZnPyr addition. Below: a trace that reflects background-subtracted fluorescence measurements of RCaMP-h normalized to GFP fluorescence *vs.* time in the given neuronal ROI, both before and after ZnPyr addition. Colour-coded dotted-line boxes (grey, PRE; red, POST) on trace segments correlate with the rainbow-contrast images above. Scale bars: vertical = 0.1 RU; horizontal = 60 s. *B*, structure is identical to Fig. 4*A*; neurons were pre and co-treated with ryanodine (15 μM) during ZnPyr treatment. *C*, before and after plots, showing the number of Ca^{2+} transients min^{-1} for ~10 min before and after ZnPyr-treatment in both control and ryanodine-supplemented conditions, as well as the pooled mean ± SEM of the data (Pre-ZnPyr, 0.84 ± 0.23, $n = 10$; Post-ZnPyr, 1.65 ± 0.37, $n = 10$; Pre-ZnPyr + ryanodine, 0.43 ± 0.15, $n = 8$; Post-ZnPyr + ryanodine, 0.47 ± 0.20, $n = 8$). Each paired data set (pre-/post-treatment) is analysed via a paired *t* test (two-tailed) (*$P < 0.05$).

In the present study, we first confirm our hypothesis that increases in intracellular Zn^{2+} are alone sufficient for Kv2.1 channel declustering. An acute surge in intracellular Zn^{2+} concentration induces transient Kv2.1 channel diffusion in the membrane. This localization change is accompanied by a small but significant hyperpolarizing shift in the voltage-gated activation kinetics of the channel. Because intracellular Zn^{2+} is an adequate preconditioning stimulus at similar concentrations (Aras *et al.* 2009*b*), capable of promoting neuronal tolerance (i.e. prevention of cell death) *in vitro*, our results further associate Kv2.1 modulation with the induction of neuronal tolerance. Importantly, we show that Zn^{2+}-mediated channel declustering is dependent on activation of calcineurin, which is a protein phosphatase known to dephosphorylate Kv2.1 at several intracellular residues (Misonou *et al.* 2004; Misonou *et al.* 2005*b*; Mulholland *et al.* 2008; Baver and O'Connell, 2012; Shah *et al.* 2014). We also found that calcineurin activation in this context is probably promoted by Ca^{2+} liberation from intracellular stores following direct modulation of neuronal RyRs by Zn^{2+}. As mentioned earlier, a recent study demonstrated direct activation of cardiac isoform RyR in myocytes by Zn^{2+} (Woodier *et al.* 2015). The present study indicates that intracellular Zn^{2+} also probably activates neuronal RyRs, linking intracellular Zn^{2+} surges to calcineurin activation. Our results therefore suggest that this process of ryanodine receptor activation may be a ubiquitous component of Zn^{2+} signalling, further solidifying the status of Zn^{2+} as an important second messenger in a large array of cell types (Yamasaki *et al.* 2007).

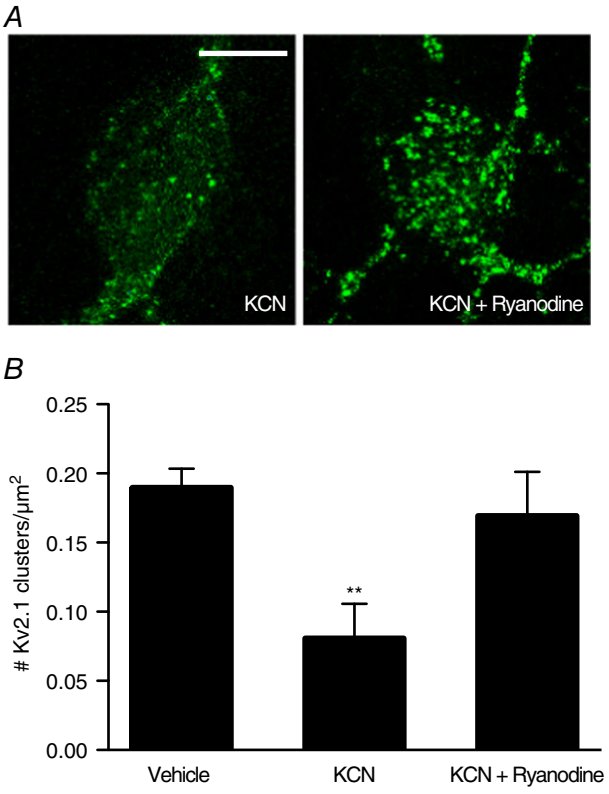

Figure 5. RyR activation by intracellular Zn^{2+} is critical to Kv2.1 channel cluster dispersal in the chemical ischaemic preconditioning pathway
A, confocal images of cortical neurons transfected with a GFP-tagged Kv2.1 construct, representative of Kv2.1 localization following treatment with either Vehicle (ddH_2O, DMSO), KCN (3 mM KCN, DMSO) or KCN + ryanodine (3 mM KCN, 15 μM ryanodine) conditions for 90 min. Prior to treatment, neuronal cultures were incubated with either vehicle or ryanodine-containing treatment solutions, depending on the treatment condition. Control images not relevant to this finding were omitted; Vehicle-treated neurons showed significant Kv2.1 channel clustering. Scale bar = 10 μm. *B*, showing the mean number of Kv2.1 clusters found in each condition, normalized to neuronal somatic area (number of Kv2.1 clusters μm^{-2} of neuronal soma). Data are shown for each condition as the mean ± SEM (Vehicle, 0.190 ± 0.014, $n = 11$; KCN, 0.081 ± 0.025, $n = 11$; KCN + ryanodine, 0.169 ± 0.032, $n = 10$). Analysed via one-way ANOVA with Dunnett's MCT *vs.* vehicle-treated neurons (**$P < 0.01$).

Recent studies have also provided strong evidence indicating that RyR and Kv2.1 are spatially linked. Indeed, accumulated RyR clusters on subsurface cER cisternae are closely apposed to plasma membrane Kv2.1 clusters, even taking the same morphological organization into clusters (Mandikian *et al.* 2014). Additionally, cER, which is an important source of cytosolic Ca^{2+} release from RyR, is closely associated with Kv2.1, such that the loss of Kv2.1 cluster-cER membrane junctions also results in dissociation of surface Kv2.1 channel clusters (Fox *et al.* 2015). Indeed, Kv2.1 channel clusters may represent the *de facto* anchor that facilitates the close apposition of the plasma membrane with the cER (Fox *et al.* 2013), with Kv2.1 surface clusters serving as an important membrane insertion point of new potassium channels, including Kv2.1 (Deutsch *et al.* 2012). Furthermore, because Kv2.1 surface clusters have been shown to be non-conducting, with declustered Kv2.1 channels mediating the majority of high threshold K^+ currents (O'Connell *et al.* 2010), these clusters probably serve a function outside of K^+ current conduction. Because we have found that Zn^{2+}-induced Kv2.1 declustering is critically reliant on a signalling mechanism involving neuronal RyR activation and Ca^{2+} liberation, the close association of RyR-containing cER to Kv2.1-containing plasma membrane clusters suggests the existence of a classical signalling microdomain (Hoessli *et al.* 2000) that enables the channel modulation observed in the present study. In this way, active molecular complexes necessary for Kv2.1 modulations are probably juxtaposed to channel clusters in a confined cytosolic environment (Fig. 6).

Thus, our model (Fig. 6) suggests that intracellular Zn^{2+} transiently alters Kv2.1 channel function and localization by direct modulation of the neuronal RyR in a highly compartmentalized mechanism. By associating

with closely apposed RyR clusters, intracellular Zn^{2+} ions mediate an increased frequency of Ca^{2+} release events from the cER in contact with Kv2.1 channel clusters on the somatic membrane. This cytosolic Ca^{2+} then rapidly binds a closely associated calcineurin-calmodulin complex, engaging protein phosphatase activity. In turn, active calcineurin dephosphorylates Kv2.1, leading, in the case reported in the present study, to a small hyperpolarizing shift in the channel's activation kinetics, perhaps aiding neurons with homeostatic adaptation to increased excitation, such as that occurring during excitotoxic injury (Aras *et al.* 2009*b*; Aras *et al.* 2009*a*; Mohapatra *et al.* 2009; Shepherd *et al.* 2013). Moreover, this profound, Zn^{2+}-dependent change in Kv2.1 may also serve as an adaptive response to injury by preventing the insertion of additional Kv2.1 channels, a phenomenon that has been tightly linked to neuronal cell death (Pal *et al.* 2003; Pal *et al.* 2006). Notably, we also demonstrate Zn^{2+}dependent activation of RyR is an important component of ischaemic preconditioning-induced changes in Kv2.1 localization, which also causes a similar increase in free cytosolic Zn^{2+}. It is important to note, overall, that this process probably proceeds in a concerted and spatially linked mechanism where Kv2.1 clusters, subsurface cER cisternae, RyR-mediated Ca^{2+} transients and calcineurin are closely associated in a signalling microdomain, allowing a kinetically fast interaction to occur. Interestingly, the calcineurin-mediated hyperpolarizing shift that we observed in the activation kinetics of Kv2.1 also exists in the presence of 11 mM EGTA in whole-cell patch pipettes; thus, this is probably not a process dependent on global Ca^{2+} release or a kinetically slow signalling mechanism. Indeed, the diminished magnitude of this hyperpolarizing shift, when compared with previously reported values closer to 20 mV (Misonou *et al.* 2005*b*), may be partially explained by the presence of this slow Ca^{2+} chelator.

In sum, intracellular Zn^{2+} has been strongly indicated as a transient, early and crucial signalling ion active in response to cellular injury, preceding cytosolic Ca^{2+} liberation. Although Zn^{2+}-dependent Ca^{2+} increases have been previously shown to occur in neurons (Medvedeva *et al.* 2009; Johanssen *et al.* 2015), the mechanism behind this process had not been defined. Specifically, the link

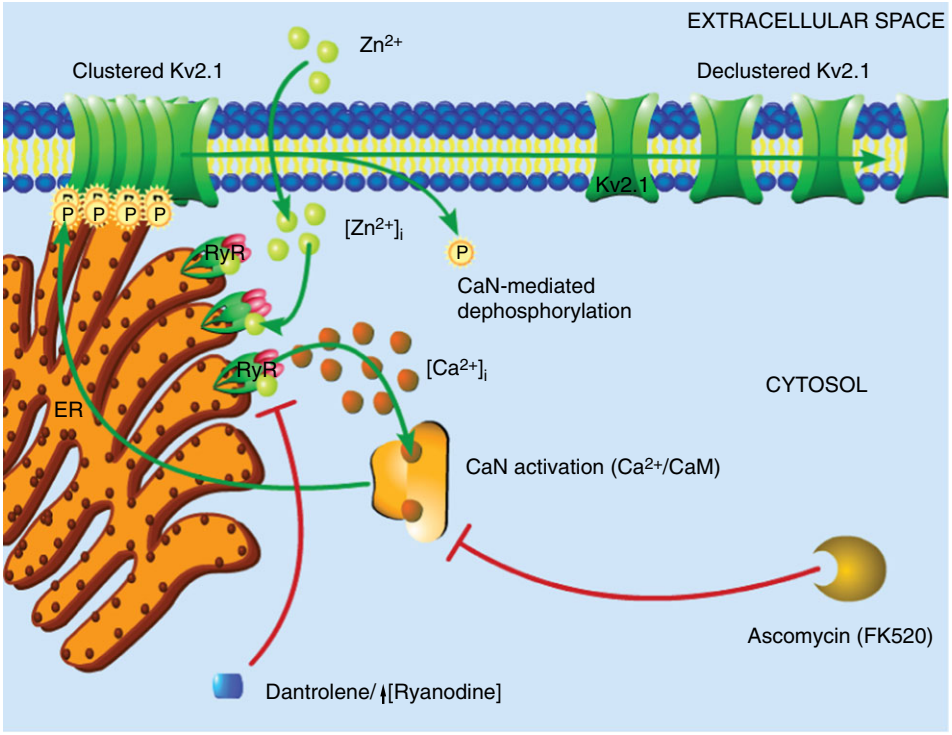

Figure 6. Intracellular Zn^{2+}-induced Kv2.1 channel modulation occurs in compartmentalized signalling domains
The results of the present study suggest that Zn^{2+} plays an early, critical role in Kv2.1 modulation. Transient surges in free Zn^{2+} concentration within the cell (either produced by exogenous ZnPyr treatment, as shown here, or induced by sublethal ischaemic injury), probably modulate neuronal RyR directly, inducing an increased Ca^{2+} event frequency. These Ca^{2+} transients, located in close proximity to Kv2.1 channel cluster domains, lead to calcineurin activation and subsequent Kv2.1 dephosphorylation and dispersal of channel localization. This signalling cascade is sensitive to Zn^{2+} chelation, calcineurin activation and RyR activity, with direct Zn^{2+}-modulation of RyR being the key link in this process between acute surges in intracellular Zn^{2+} and calcineurin-mediated Kv2.1 modulation.

between Zn^{2+} and Ca^{2+} had not been clarified. The present study provides a critical, mechanistic link between intracellular Zn^{2+} signalling and RyR-dependent cytosolic Ca^{2+} liberation leading to Kv2.1 declustering and cellular adaptive responses. As such, Zn^{2+} may well be a ubiquitous signalling ion in the central nervous system, critically regulating neuronal function and cellular homeostasis in response to a wide range of environmental insults.

References

Akerboom J, Calderón NC, Tian L, Wabnig S, Prigge M, Tolö J, Gordus A, Orger MB, Severi KE & Macklin JJ (2013). Genetically encoded calcium indicators for multi-color neural activity imaging and combination with optogenetics. *Front Mol Neurosci* **6**, 2.

Aras MA, Saadi RA & Aizenman E (2009*a*). Zn^{2+} regulates Kv2. 1 voltage-dependent gating and localization following ischemia. *Eur J Neurosci* **30**, 2250–2257.

Aras MA, Hara H, Hartnett KA, Kandler K & Aizenman E (2009*b*). Protein kinase C regulation of neuronal zinc signaling mediates survival during preconditioning. *J Neurochem* **110**, 106–117.

Baver SB & O'Connell KM (2012). The C-terminus of neuronal Kv2. 1 channels is required for channel localization and targeting but not for NMDA-receptor-mediated regulation of channel function. *Neuroscience* **217**, 56–66.

Besser L, Chorin E, Sekler I, Silverman WF, Atkin S, Russell JT & Hershfinkel M (2009). Synaptically released zinc triggers metabotropic signaling via a zinc-sensing receptor in the hippocampus. *J Neurosci* **29**, 2890–2901.

Deutsch E, Weigel AV, Akin EJ, Fox P, Hansen G, Haberkorn CJ, Loftus R, Krapf D & Tamkun MM (2012). Kv2. 1 cell surface clusters are insertion platforms for ion channel delivery to the plasma membrane. *Mol Biol Cell* **23**, 2917–2929.

Du J, Haak LL, Phillips-Tansey E, Russell JT & McBain CJ (2000). Frequency-dependent regulation of rat hippocampal somato-dendritic excitability by the K^+ channel subunit Kv2. 1. *J Physiol* **522**, 19–31.

Fox PD, Loftus RJ & Tamkun MM (2013). Regulation of Kv2. 1 K^+ conductance by cell surface channel density. *J Neurosci* **33**, 1259–1270.

Fox PD, Haberkorn CJ, Akin EJ, Seel PJ, Krapf D & Tamkun MM (2015). Induction of stable endoplasmic reticulum/plasma membrane junctions by Kv2. 1 potassium channels. *J Cell Sci* **128**, 2096–2105.

Frederickson CJ, Koh J-Y & Bush AI (2005). The neurobiology of zinc in health and disease. *Nat Rev Neurosci* **6**, 449–462.

Gomez-Hurtado N, Oo YW, Laver D & Knollmann B (2014). Presence of calmodulin potentiates block of ryanodine receptor calcium release channels by dantrolene and flecainide. *Circulation* **130**, A18157–A18157.

Granzotto A & Sensi SL (2015). Intracellular zinc is a critical intermediate in the excitotoxic cascade. *Neurobiol Dis* **81**, 25–37.

Grundy D (2015). Principles and standards for reporting animal experiments in *The Journal of Physiology* and *Experimental Physiology*. *Exp Physiol* **100**, 755–758.

Hartnett K, Stout A, Rajdev S, Rosenberg P, Reynolds I & Aizenman E (1997). NMDA Receptor-mediated neurotoxicity: a paradoxical requirement for extracellular Mg^{2+} in Na^+/Ca^{2+}-free solutions in rat cortical neurons in vitro. *J Neurochem* **68**, 1836–1845.

Hoessli DC, Ilangumaran S, Soltermann A, Robinson PJ & Borisch B (2000). Signaling through sphingolipid microdomains of the plasma membrane: the concept of signaling platform. *Glycoconj J* **17**, 191–197.

Johanssen T, Suphantarida N, Donnelly PS, Liu XM, Petrou S, Hill AF & Barnham KJ (2015). PBT2 inhibits glutamate-induced excitotoxicity in neurons through metal-mediated preconditioning. *Neurobiol Dis* **81**, 176–185.

Lim ST, Antonucci DE, Scannevin RH & Trimmer JS (2000). A novel targeting signal for proximal clustering of the Kv2. 1 K^+ channel in hippocampal neurons. *Neuron* **25**, 385–397.

Lotem J, Kama R & Sachs L (1999). Suppression or induction of apoptosis by opposing pathways downstream from calcium-activated calcineurin. *Proc Natl Acad Sci USA* **96**, 12016–12020.

Mandikian D, Bocksteins E, Parajuli LK, Bishop HI, Cerda O, Shigemoto R & Trimmer JS (2014). Cell type-specific spatial and functional coupling between mammalian brain Kv2. 1 K^+ channels and ryanodine receptors. *J Comp Neurol* **522**, 3555–3574.

Medvedeva YV, Lin B, Shuttleworth CW & Weiss JH (2009). Intracellular Zn^{2+} accumulation contributes to synaptic failure, mitochondrial depolarization, and cell death in an acute slice oxygen-glucose deprivation model of ischemia. *J Neurosci* **29**, 1105–1114.

Misonou H, Mohapatra DP & Trimmer JS (2005*a*). Kv2. 1: a voltage-gated K^+ channel critical to dynamic control of neuronal excitability. *Neurotoxicology* **26**, 743–752.

Misonou H, Mohapatra DP, Menegola M & Trimmer JS (2005*b*). Calcium- and metabolic state-dependent modulation of the voltage-dependent Kv2. 1 channel regulates neuronal excitability in response to ischemia. *J Neurosci* **25**, 11184–11193.

Misonou H, Mohapatra DP, Park EW, Leung V, Zhen D, Misonou K, Anderson AE & Trimmer JS (2004). Regulation of ion channel localization and phosphorylation by neuronal activity. *Nat Neurosci* **7**, 711–718.

Mohapatra DP & Trimmer JS (2006). The Kv2. 1 C terminus can autonomously transfer Kv2. 1-like phosphorylation-dependent localization, voltage-dependent gating, and muscarinic modulation to diverse Kv channels. *J Neurosci* **26**, 685–695.

Mohapatra DP, Misonou H, Sheng-Jun P, Held JE, Surmeier DJ & Trimmer JS (2009). Regulation of intrinsic excitability in hippocampal neurons by activity-dependent modulation of the KV2. 1 potassium channel. *Channels* **3**, 46–56.

Mulholland PJ, Carpenter-Hyland EP, Hearing MC, Becker HC, Woodward JJ & Chandler LJ (2008). Glutamate transporters regulate extrasynaptic NMDA receptor modulation of Kv2. 1 potassium channels. *J Neurosci* **28**, 8801–8809.

O'Connell KM, Loftus R & Tamkun MM (2010). Localization-dependent activity of the Kv2. 1 delayed-rectifier K^+ channel. *Proc Natl Acad Sci USA* **107**, 12351–12356.

O'Connell KM, Rolig AS, Whitesell JD & Tamkun MM (2006). Kv2. 1 potassium channels are retained within dynamic cell surface microdomains that are defined by a perimeter fence. *J Neurosci* **26**, 9609–9618.

Pal S, Takimoto K, Aizenman E & Levitan E (2006). Apoptotic surface delivery of K^+ channels. *Cell Death Differ* **13**, 661–667.

Pal S, Hartnett KA, Nerbonne JM, Levitan ES & Aizenman E (2003). Mediation of neuronal apoptosis by Kv2. 1-encoded potassium channels. *J Neurosci* **23**, 4798–4802.

Park K-S, Mohapatra DP, Misonou H & Trimmer JS (2006). Graded regulation of the Kv2. 1 potassium channel by variable phosphorylation. *Science* **313**, 976–979.

Scannevin RH, Murakoshi H, Rhodes KJ & Trimmer JS (1996). Identification of a cytoplasmic domain important in the polarized expression and clustering of the Kv2. 1 K^+ channel. *J Cell Biol* **135**, 1619–1632.

Sensi SL, Paoletti P, Koh J-Y, Aizenman E, Bush AI & Hershfinkel M (2011). The neurophysiology and pathology of brain zinc. *J Neurosci* **31**, 16076–16085.

Shah NH & Aizenman E (2014). Voltage-gated potassium channels at the crossroads of neuronal function, ischemic tolerance, and neurodegeneration. *Transl Stroke Res* **5**, 38–58.

Shah NH, Schulien AJ, Clemens K, Aizenman TD, Hageman TM, Wills ZP & Aizenman E (2014). Cyclin E1 regulates Kv2. 1 channel phosphorylation and localization in neuronal ischemia. *J Neurosci* **34**, 4326–4331.

Shepherd AJ, Loo L & Mohapatra DP (2013). Chemokine co-receptor CCR5/CXCR4-dependent modulation of Kv2. 1 channel confers acute neuroprotection to HIV-1 glycoprotein gp120 exposure. *PloS ONE* **8**, e76698.

Shepherd AJ, Loo L, Gupte RP, Mickle AD & Mohapatra DP (2012). Distinct modifications in Kv2. 1 channel via chemokine receptor CXCR4 regulate neuronal survival-death dynamics. *J Neurosci* **32**, 17725–17739.

Surmeier DJ & Foehring R (2004). A mechanism for homeostatic plasticity. *Nat Neurosci* **7**, 691–692.

Sutko JL, Airey JA, Welch W & Ruest L (1997). The pharmacology of ryanodine and related compounds. *Pharmacol Rev* **49**, 53–98.

Tamkun MM, O'Connell KM & Rolig AS (2007). A cytoskeletal-based perimeter fence selectively corrals a sub-population of cell surface Kv2. 1 channels. *J Cell Sci* **120**, 2413–2423.

Woodier J, Rainbow RD, Stewart AJ & Pitt SJ (2015). Intracellular zinc modulates cardiac ryanodine receptor-mediated calcium release. *J Biol Chem* **290**, 17599–17610.

Yamasaki K, Kigawa T, Watanabe S, Inoue M, Yamasaki T, Seki M, Shinozaki K & Yokoyama S (2012). Structural basis for sequence-specific DNA recognition by an *Arabidopsis* WRKY transcription factor. *J Biol Chem* **287**, 7683–7691.

Yamasaki S, Sakata-Sogawa K, Hasegawa A, Suzuki T, Kabu K, Sato E, Kurosaki T, Yamashita S, Tokunaga M & Nishida K (2007). Zinc is a novel intracellular second messenger. *J Cell Biol* **177**, 637–645.

Additional information

Competing interests

The authors declare that they have no competing interests.

Author contributions

AJS, NHS, JAJ, RDM, ZPW and EA designed the research. AJS, NHS, JAJ, RDM and ZPW collected data. AJS, NHS, JAJ, RDM, ZPW and EA analysed and interpreted data. AJS, NHS, JAJ and EA wrote the manuscript. EA provided financial support. ZPW provided some reagents and materials. All authors have approved the final version of the manuscript and agree to be accountable for all aspects of the work. All persons designated as authors qualify for authorship, and all those who qualify for authorship are listed.

Funding

This work was supported by NIH grant NS043277 to EA. NHS was supported by the American Heart Association Pre-doctoral Fellowship 12PRE11070001. JAJ is supported by NIH T32 NS086749.

Acknowledgements

We thank D. P. Mohapatra, Washington University, St Louis, for GFP-Kv2.1-expressing plasmid; C. A. Anderson for helpful suggestions; and K. A. Hartnett for technical support.